Nanomagnetic Logic: Error-Free, Directed Signal Transmission by an Inverter Chain

I. Eichwald[1], A. Bartel[1], J. Kiermaier[1], S. Breitkreutz[1], G. Csaba[2], D. Schmitt-Landsiedel[1], and M. Becherer[1]

[1]Theresienstraße 90/Rückgebäude N3, München 80333, Germany
[2]224 Cushing Hall, Notre Dame, IN 46556 USA

In this paper we present a new clocking method for non-reciprocal information transmission by an inverter chain of focused ion-beam engineered Co/Ni nanomagnets. The functionality of the clocking method is proven experimentally. Local focused ion-beam irradiation is used in order to define the direction of the information flow. The nanodots of the chain are clocked synchronously by a global external field. Information is transmitted synchronously between neighboring dots due to field-coupling. Magnetic force microscopy is used to reveal the magnetization state of the nanomagnets after every field pulse to prove the correct transmission of the signal. The switching characteristics of the fabricated nanodots and coupling forces between neighboring dots are analyzed optically using the magneto-optical Kerr effect. A detailed explanation is given for the occurrence of possible errors in a field coupled inverter chain.

***Index Terms*—Cobalt, magnetic logic devices, nickel, perpendicular magnetic anisotropy.**

I. Introduction

Nanomagnetic logic (NML) is attracting more and more attention due to its potential benefits: ultra-low power computing, non-volatility, radiation hardness, ultra-high density data storage and processing. This technology (also known as magnetic quantum cellular automata (MCQA)) can complement CMOS-based circuitry [1] as it enables logic and memory functions in the same device. We investigate NML possessing perpendicular magnetic anisotropy (PMA) as PMA is known to be advantageous for field-coupled architectures [1]. These advantages are scalability, design space in shape and definable directed signal flow by the predefined placement of focused ion-beam (FIB) irradiation. Such nanomagnets show an out-of-plane bistable magnetization. The magnetization direction is encoded with the Boolean logic states '0' and '1'. Two neighboring dots interact via field-coupling enabling digital information flow. Complex gates like NOT, NOR and NAND can be realized by a certain spatial arrangement of nanomagnets as envisioned in [2], [3]. For the injection of information an electrical input can be used as proposed in [4]. In [5] an electrical output is demonstrated for the read-out of the magnetization state of the output nanomagnet. In Fig. 1(a) a schematic design of a nanomagnetic, computing system is depicted. The transmission of information between logic gates operates via field-coupled nanomagnetic chains. For this purpose a clocking system is required which enables directed and error-free signal transmission in such magnetic wires. In [6], a nanomagnetic wire has already been realized by nanomagnets with in-plane magnetization using an adiabatic hard-axis clocking field.

In this paper a new clocking method is presented and demonstrated for an inverter chain of Co/Ni nanomagnets with PMA. To set the magnetization of the first dot in the chain a current driven wire can be used to generate a magnetic field acting as electrical input. All dots are clocked synchronously by an external magnetic field in easy-axis (out-of-plane) direction. After every field pulse, information is transmitted one dot further. The superposition of the external field and the dipole field of the previous dot sets the magnetization state of the following dot (see Fig. 1(b)). The global field can be generated by integrated inductors or coils in the package. After two clocking cycles new information can be injected in the chain by the input, acting like a pipeline. In order to define the information flow the dots were partially irradiated by the FIB.

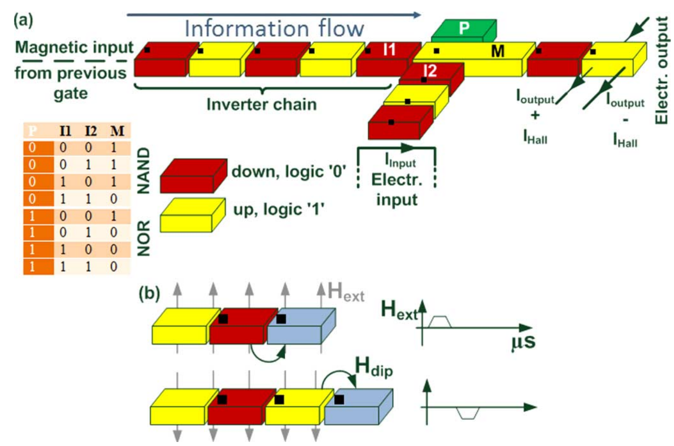

Fig. 1. (a) Schematic design of a field-coupled nanomagnetic system, with an electrical in- and output, an inverter chain and a hard-magnetic programmable dot P. The magnetic state of dot P sets the functionality of the majority gate acting as NAND or NOR device. The black rectangles indicate the irradiation area of the FIB. (b) Schematic design of the clocking system.

In our earlier experiments Co/Pt nanomagnets were used. For an error-free information transmission high coupling fields are advantageous. Therefore we investigated a new material stack of Co/Ni. As Ni is ferromagnetic the saturation magnetization in the stack could be increased and thereby also the coupling. Furthermore Co/Ni dots show lower switching fields in comparison to Co/Pt dots due to reduced anisotropy. Hence, lower magnitude clocking fields can be used and therefore the power consumption of the system is decreased. To ensure error-free

Manuscript received March 02, 2012; accepted April 12, 2012. Date of current version October 19, 2012. Corresponding author: I. Eichwald (e-mail: irina.eichwald@tum.de).

Color versions of one or more of the figures in this paper are available online at http://ieeexplore.ieee.org.

Digital Object Identifier 10.1109/TMAG.2012.2196030

information flow high thermal stability, small dot to dot variations and strong coupling fields are required. Our measurements prove that Co/Ni dots meet these requirements.

II. Theory

The considered inverter chain consists of Co/Ni dots. Our clocking method employs alternating global magnetic field pulses in easy-axis direction. The magnets are clocked synchronously by the field amplitude $\mathrm{H_{pulse}}$ and information is transmitted sequentially from dot to dot due to field-coupling. For the determination of $\mathrm{H_{pulse}}$ the following crucial factors have to be taken into account:

a) *Coupling k*
b) *Placement of FIB irradiation*
c) *Thermal noise*
d) *Dot to dot variations in the fabrication process*

A. Influence of Coupling K

The strength of the stray field of a nanomagnet that acts on a neighboring dot and forces it into antiparallel alignment is expressed by the coupling k. It influences the former or subsequent switching of a coupled neighboring dot. Consider two neighboring dots having different switching fields. Dot1 has a higher switching field than Dot2. Both are magnetized in one direction (initial state). By applying an external field against the magnetization direction the stray field of Dot1 helps the external field to switch the neighboring Dot2 into antiparallel alignment. Dot2 will already switch at a lower field value $\mu_0\mathrm{H_{C,Dot2}} - \mathrm{k}$ than without the interaction of the stray field of Dot1. To reverse the magnetization of Dot2 back in the initial state, a higher field value $\mu_0\mathrm{H_{C,Dot2}} + \mathrm{k}$ is required as the stray field of Dot1 stabilizes the antiparallel alignment and now counteracts the external field. Hence, the hysteresis loop of Dot2 is shifted by two times the coupling k depending on the magnetization state of Dot1. This impact of k on the switching field of Dot2 is sketched in Fig. 2. As the stray field gets weaker with increasing distance to the dot's edge, the interdot distance is significant for the coupling. The coupling can be improved by increasing the area-specific saturation magnetization:

$$\mathrm{M_S} \cdot \mathrm{t} = (\mathrm{M_{S,Co}} \cdot \mathrm{t_{Co}} + \mathrm{M_{S,Ni}} \cdot \mathrm{t_{Ni}}) \cdot \mathrm{N} \tag{1}$$

with $\mathrm{M_{S,Co}} = 14.4 \cdot 10^5$ A/m and $\mathrm{M_{S,Ni}} = 5.1 \cdot 10^5$ A/m being the saturation magnetization of Co and Ni, $\mathrm{t_{Co}}$ and $\mathrm{t_{Ni}}$ being the layer thickness of Co and Ni and N being the bilayer number of the considered film. As $\mathrm{M_{S,Ni}} \approx 1/3 \cdot \mathrm{M_{S,Co}}$, the amount of Co in the film stack mainly influences the saturation magnetization.

B. Placement of FIB Irradiation

During the switching process the magnetization reversal of the coupled dot always starts at a point with lowest anisotropy in the dot. In this area the stray field of the neighboring dot has the most influence to set the right magnetization state. The closer this point is situated to the dot's edge the more probable is the switching of the coupled dot in the antiparallel and therefore in the correct state. After the fabrication of the dots, this weakest point in the dot can be set by FIB irradiation. Irradiating a small area in the dot, the anisotropy in this area is destroyed and an artificial nucleation center for a domain wall is created [7]. During

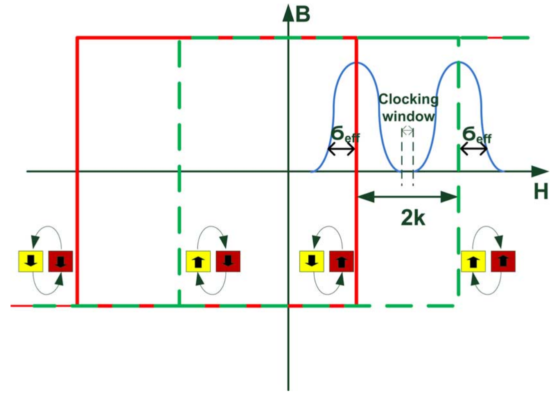

Fig. 2. Hysteresis loops of the coupled dot Dot2. Depending on the magnetization state of Dot1 the hysteresis loops for Dot2 are shifted by two times the coupling k.

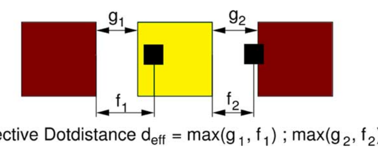

Fig. 3. Effective Dot distance $\mathrm{d_{eff}}$ being the maximum of the nominal interdot distance g and the distance of the irradiated area to the dot's edge f. The black squares indicate the irradiated area in the dot.

the switching process, the domain wall motion starts in this predefined area and propagates through the whole dot. The nearer the irradiated area is situated to the dot's edge the stronger is the stray field that acts on this weak spot of the dot. Hence, the effective distance $\mathrm{d_{eff}}$ determining the coupling is the maximum of the nominal interdot distance g and the distance of the irradiation to the dot's edge f as sketched in Fig. 3. Therefore the placement of this artificial nucleation center is another crucial point for error-free signal propagation.

As a result of the FIB irradiation the direction of the signal flow is also predefined. In [8], experiments have been done to show the dependence of the propagation direction on the placement of the irradiated area on the dot. There three dots were placed together in a row separated by a distance of about 100 nm. The middle dot was irradiated on its left edge. The measurements have shown that the magnetization state of this middle dot was only sensible to the magnetization state of its left neighbor. This experiment demonstrated that the signal was transmitted from left to right and not backwards.

As an additional effect, FIB irradiation significantly reduces the switching field of the nanomagnets, which is crucial for the power consumption of the system.

C. Thermal Noise & D) Dot to Dot Variations in the Fabrication Process

Thermal noise and variations in the fabrication process are the two effects influencing the switching field distribution (SFD) of a dot. The switching field $\mathrm{H_C}$ of a nanomagnet is normal distributed over time due to thermal noise [9]. So we get a first variational range for the field at which a dot may switch. A second range is given by the variations in the fabrication process. Here $\mathrm{H_C}$ varies from dot to dot. These variations are also normal distributed [10]. Both distributions have to be convoluted to get the switching field distribution for the dots in the chain:

$$\mathbf{SFD}_{\mathrm{eff}} = \mathbf{SFD}_{\mathrm{T}} * \mathbf{SFD}_{\mathrm{Fab}}. \tag{2}$$

In Fig. 2 the convoluted switching field distribution due to thermal noise and variations in the fabrication process is indicated by $\boldsymbol{\sigma}_{\mathrm{eff}}$. In sum, we get a broadened distribution of $\mathrm{H_C}$ separated by twice the coupling. The field values between the shifted distributions can be used to clock the system, called the clocking window.

D. Summary

Both, thermal noise and variations in the fabrication process broaden the switching field distribution and therefore diminish the clocking window. A higher coupling broadens the clocking window. The influence of the coupling can be promoted by the correct placement of FIB irradiation.

III. Experimental Setup

A. Dot Fabrication

Sub-nanometer thick Co and Ni layers were sputtered on top of a silicon substrate. The nanomagnets were defined by FIB lithography on a PMMA photoresist followed by ion beam etching (IBE). Cr is used as hard mask for the etching process. Afterwards the hard mask is removed by Cr wet etching. The film stack is composed as following $\mathrm{Ti_{2nm}\ Au_{10nm}\ Pt_{5nm}8x[Co_{0.2nm} + Ni_{0.4nm}]Pt_{5nm}}$. This corresponds to a $\mathrm{M_S} \cdot \mathrm{t} = 3.94$ mA. After sputtering, the sample is annealed at 200°C on a hotplate for at least thirty minutes to get PMA. Longer annealing times are not advisable, as measurements of the hysteresis curve have shown a less sharp switching behavior of samples with very long annealing times. An annealing over 200°C is critical because higher temperatures cause losses in the saturation magnetization and higher switching fields are induced [11].

B. FIB Irradiation

In order to define the direction of information flow in the inverter chain from left to right, the dots were FIB irradiated at their left edge by a dose of $1 \cdot 10^{14}$ Ions/cm^2. The irradiation area is $80 \cdot 80$ nm^2.

IV. Results

A. MOKE Measurements

In the following the magnetic properties of the fabricated nanomagnets are analyzed. For the investigation of the thermal effects on the Co/Ni nanomagnets, one dot was switched over two hundred times while $\mathrm{H_C}$ was measured with the MOKE. We measured a SFD with $\boldsymbol{\sigma}_{\mathrm{T}} = 0.91$ mT. Variations in the fabrication process also cause a distribution in the switching field from dot to dot. Therefore the switching behavior of twenty dots of one Co/Ni film was analyzed. A SFD with mean $\mu_0\ \mathrm{H_{C,mean}} = 58.42$ mT and $\boldsymbol{\sigma}_{\mathrm{Fab}} = 6.75$ mT (after FIB irradiation) was measured. The reduction factor of $\mu_0\ \mathrm{H_{C,mean}}$ due to FIB irradiation was 4. For the investigation of the coupling, k was measured for twenty dot pairs that are shown in Fig. 4(a). The measurements of k revealed $\mathrm{k} = 6$ mT for a nominal interdot distance of 60 nm as shown in Fig. 4(b). As the irradiation area is $80 \cdot 80$ nm^2 and we assume that the nucleation of the domain wall starts right in the middle of this area, the effective distance to the dot's edge is $\mathrm{d_{eff}} = 100$ nm.

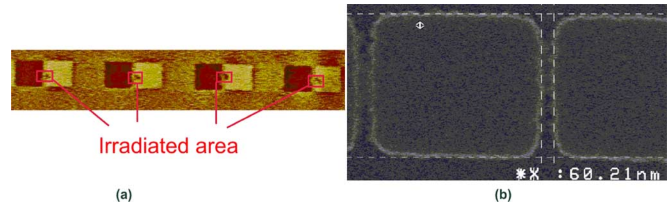

Fig. 4. (a) MFM phase image of Co/Ni dot pairs whereas the right neighbor dot is irradiated by the FIB. (b) SEM image of the nominal interdot distance.

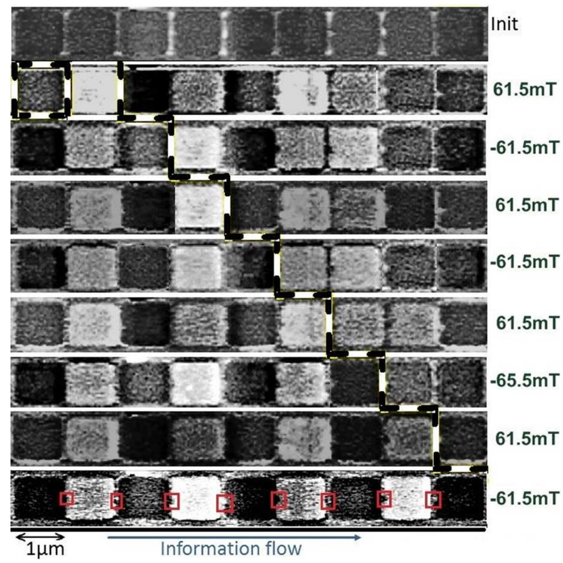

Fig. 5. MFM phase image of the signal transmission marked by the dashed line. On the right site the required $\mathrm{H_{pulse}}$ is denoted. After every pulse information is transmitted one dot further. Additionally, in the last line the irradiated areas of the dots are marked by the red rectangles.

B. MFM Demonstration

In the following the new clocking method is analyzed for the inverter chain of the Co/Ni dots investigated in the previous section. Magnetic force microscopy reveals the states of the nanomagnets after every clocking pulse in Fig. 5. The dashed line marks the propagation of information. The input dot is also marked by the dashed line. The information flow is from left to right. In the initial state of the inverter chain all dots show a downward magnetization. First a positive pulse is applied. The stray field of the input dot helps the external field to switch the neighboring dot into antiparallel alignment. After the alignment a negative pulse is applied. Now the stray field of the second dot in the chain contributes to switch the third dot in the correct state. Furthermore the magnetization state of the second dot is not affected by the opposed external field as this dot is stabilized by the stray field of the input dot. After every field pulse the information propagates one dot further. For the determination of the optimum $\mathrm{H_{pulse}}$, different field amplitudes were tested. $\mu_0\ \mathrm{H_{pulse}} = \pm 61.5$ mT was determined to switch all the dots in the correct state except one. Between the 6th and 7th dot a frustration occurs attributed to smaller field coupling. Here a higher field had to be applied to switch the dot in the correct configuration. Note, that the already ordered dots were not affected by this higher field. For the last two following dots this field strength was too high and the external field had to be reduced again. These measurements have shown that it was not possible

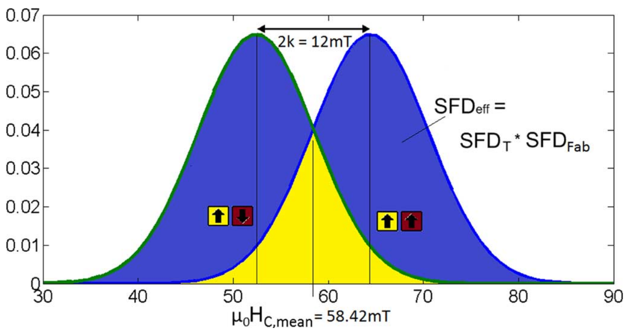

Fig. 6. SFDs shifted two times by the coupling k. Due to the overlap between both distributions there is no sufficient clocking window for $\mathrm{d_{eff}} = 100$ nm.

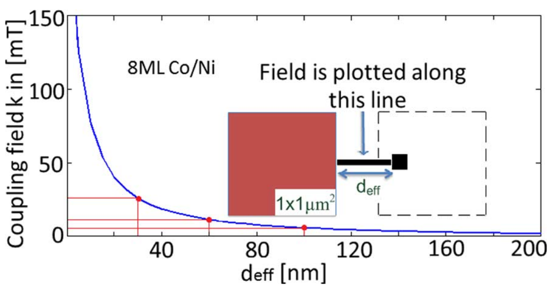

Fig. 7. OOMMF Simulation for the coupling k of one dot. For $\mathrm{d_{eff}} = 100$ nm: $\mathrm{k} = 5.7$ mT, for $\mathrm{d_{eff}} = 60$ nm: $\mathrm{k} = 11.5$ mT and for $\mathrm{d_{eff}} = 30$ nm: $\mathrm{k} = 26.5$ mT.

to clock this inverter chain correctly using one and the same $\mathrm{H_{pulse}}$.

The reasons are sketched in Fig. 6. As already mentioned in the theory section, thermal noise and variation in the fabrication process cause a SFD of the dots. Summing up the SFDs of all dots of the inverter chain we got a broadened $\mathrm{SFD_{eff}}$. The switching field of a dot is shifted by the coupling field $\pm$ k depending on the magnetization state of its previous dot. Therefore we get two Gaussian distributions separated by twice the coupling field. If coupling is not high enough both distributions overlap and errors may occur as there is no sufficient clocking window. Shifting the distributions further apart means either enhancing the coupling or minimizing the fluctuations due to variations in the fabrication process or thermal noise. The coupling can be increased by enhancing the amount of the magnetic material in the stack, the number of multilayers or by shrinking the effective distance $\mathrm{d_{eff}}$ between dots. The influence of the distance on k and therefore on the width of the clocking window is shown in Fig. 7. We used a standard micromagnetic simulator, the OOMMF framework [12] to simulate the strength of the stray field of one dot depending on the distance to its edge. The coupling k shows a $1/\mathrm{d_{eff}}$ behavior. Hence it is crucial for the width of the clocking window. For a distance of $\mathrm{d_{eff}} = 100$ nm, k is 5.7 mT which corresponds to our value measured via MOKE. Furthermore simulations have shown that a few nanoseconds are needed to reverse the magnetization of one nanomagnet. Hence, a possible clocking frequency is 100 MHz.

V. Conclusion

A new clocking method has been presented to propagate information through an inverter chain of nanomagnets. Critical factors like the coupling, placement of FIB irradiation, switching field distributions due to thermal noise and variation in the fabrication process were analyzed in detail. Experiments have shown that error-free signal propagation over nine dots with a global external clocking field is possible. After every second clocking cycle new information can be injected in the chain allowing highly pipelined operation. Furthermore this clocking system can be used to clock simultaneously chains that are spatially arranged in parallel. Investigations on the magnetic properties of Co/Ni nanodots resulted in small switching field distributions and high coupling fields (k) being the key parameters for small error rates.

Acknowledgment

This work was supported in part by the DFG under Grants SCHM 1478/9-1 and CS 62/2-1, by DARPA-BAA-10-42 “Non-Volatile Logic,” and in part by the Technische Universität München—Institute for Advanced Study, funded by the German Excellence Initiative.

References

[1] G. Csaba, P. Lugli, M. Becherer, D. Schmitt-Landsiedel, and W. Porod, “Field-coupled computing in magnetic multilayers,” *J. Comput. Electron.*, vol. 7, pp. 454–457, 2008.

[2] G. Csaba, W. Porod, and A. I. Csurgay, “A computing architecture composed of field-coupled single-domain nanomagnets clocked by magnetic fields,” *Int. J. Circuit Theory Applicat.*, vol. 31, pp. 67–82, 2003.

[3] M. Becherer, R. Emling, W. Porod, P. Lugli, and D. Schmitt-Landsiedel, “Field-coupled nanomagnets for interconnect-free nonvolatile computing,” in *Proc. IEEE Int. Solid State Circuits Conf. (ISSCC) Digest* , 2009, pp. 474–475.

[4] J. Kiermaier, S. Breitkreutz, G. Csaba, D. Schmitt-Landsiedel, and M. Becherer, “Electrical input structures for nanomagnetic logic devices,” *J. Appl. Phys.*, to be published.

[5] J. Kiermaier, S. Breitkreutz, X. Ju, G. Csaba, D. Schmitt-Landsiedel, and M. Becherer, “Ultra-low volume ferromagnetic nanodots for field-coupled computing devices,” in *Proc. IEEE 40th Eur. Solid-State Device Research Conf. ESSDERC*, 2010, pp. 214–217.

[6] A. Imre, G. Csaba, L. Ji, A. Orlov, G. Bernstein, and W. Porod, “Majority logic gate for magnetic quantum-dot cellular automata,” *Science*, vol. 311, pp. 205–208, 2006.

[7] S. Breitkreutz, J. Kiermaier, S. V. Karthik, G. Csaba, D. Schmitt-Landsiedel, and M. Becherer, “Controlled reversal of Co/Pt dots for nanomagnetic logic applications,” *J. Appl. Phys.*, vol. 111, p. 07A715, 2012.

[8] S. Breitkreutz, J. Kiermaier, X. Ju, G. Csaba, D. Schmitt-Landsiedel, and M. Becherer, “Nanomagnetic logic: Demonstration of directed signal flow for field-coupled computing devices,” in *Proc. IEEE 41st Eur. Solid-State Device Research Conf. ESSDERC*, 2011, pp. 323–326.

[9] G. Csaba and W. Porod, “Behavior of nanomagnet logic in the presence of thermal noise,” presented at the 14th Int. Workshop on Computational Electronics (IWCE), 2010.

[10] T. Thomson, G. Hu, and B. D. Terris, “Intrinsic distribution of magnetic anisotropy in thin films probed by patterned nanostructures,” *Phys. Rev. Lett.*, vol. 96, 2006.

[11] H. Kurt, M. Venkatesan, and J. M. D. Coey, “Enhanced perpendicular magnetic anisotropy in Co/Ni multilayers with a thin seed layer,” *J. Appl. Phys.*, vol. 108, 2010.

[12] [Online]. Available: http://math.nist.gov/oommf/